© The American Society of Gene & Cell Therapy

Spinal Delivery of AAV Vector Restores Enzyme Activity and Increases Ventilation in Pompe Mice

Kai Qiu[1,2], Darin J Falk[3,4], Paul J Reier[2,5], Barry J Byrne[3,4] and David D Fuller[1,2]

[1]Department of Physical Therapy, College of Public Health and Health Professions, University of Florida, Gainesville, Florida, USA; [2]McKnight Brain Institute, University of Florida, Gainesville, Florida, USA; [3]Department of Pediatrics, Divisions of Cellular and Molecular Therapy and Pediatric Cardiology, College of Medicine, University of Florida, Gainesville, Florida, USA; [4]Powell Gene Therapy Center, University of Florida, Gainesville, Florida, USA; [5]Department of Neuroscience, College of Medicine, University of Florida, Gainesville, Florida, USA

Pompe disease is a form of muscular dystrophy due to lysosomal storage of glycogen caused by deficiency of acid α-glucosidase (GAA). Respiratory failure in Pompe disease has been attributed to respiratory muscle dysfunction. However, evaluation of spinal tissue from Pompe patients and animal models indicates glycogen accumulation and lower motoneuron pathology. We hypothesized that restoring GAA enzyme activity in the region of the phrenic motor nucleus could lead to improved breathing in a murine Pompe model (the *Gaa*$^{-/-}$ mouse). Adeno-associated virus serotype 5 (AAV5), encoding either GAA or green fluorescent protein (GFP), was delivered at the C_3–C_4 spinal level of adult *Gaa*$^{-/-}$ mice and the spinal cords were harvested 4 weeks later. AAV5-GAA injection restored spinal GAA enzyme activity and GAA immunostaining was evident throughout the cervical ventral horn. The periodic acid Schiff (PAS) method was used to examine neuronal glycogen accumulation, and spinal PAS staining was attenuated after AAV5-GAA injection. Lastly, plethysmography revealed that minute ventilation was greater in unanesthetized AAV5-GAA versus AAV5-GFP treated *Gaa*$^{-/-}$ mice at 1–4 months postinjection. These results support the hypothesis that spinal cord pathology substantially contributes to ventilatory dysfunction in *Gaa*$^{-/-}$ mice and therefore requires further detailed evaluation in patients with Pompe disease.

Received 21 April 2011; accepted 12 September 2011; published online 18 October 2011. doi:10.1038/mt.2011.214

INTRODUCTION

Deficiency of acid α-glucosidase (GAA), a lysosomal enzyme responsible for degradation of glycogen is a prominent pathological signature of the type of muscular dystrophy associated with Pompe disease. The early onset or severe form of Pompe disease is associated with complete GAA deficiency, and untreated infants often succumb to cardiorespiratory failure within the first year.[1,2] Juvenile and adult onset forms of the disease are characterized by reduced GAA activity and progressive respiratory failure.[3] Although motor problems in Pompe disease have historically been attributed to muscular pathology,[4] glycogen accumulation in the central nervous system (CNS) has been documented in Pompe tissues[5–10] and in various Pompe animal models.[5,11,12] Clinical Pompe case reports also highlight the involvement of the CNS in motor[10,13–17] and possibly cognitive deficiencies.[18] In addition, the potential contribution of the CNS to respiratory motor dysfunction has been raised by a few recent reports.[5,12,17] We recently reported that a transgenic mouse model of Pompe Disease (the *Gaa*$^{-/-}$ mouse)[19] demonstrates glycogen accumulation in phrenic motoneurons, which innervate the diaphragm (*i.e.*, the major muscle of inspiration) and reduction in ventilation.[5] Additional histological and biochemical studies of tissue obtained from a Pompe patient who suffered progressive ventilatory insufficiency revealed pathology in putative phrenic motoneurons and extensive glycogen accumulation in the spinal cord.[5] The potential for a neural substrate contribution to respiratory insufficiency in Pompe disease raises considerations about the current clinical approach involving enzyme replacement by intravenous delivery. That strategy does not lend to CNS treatment since the recombinant GAA enzyme does not cross the blood-brain-barrier.[20,21] Accordingly, Pompe patients undergoing enzyme replacement therapy would continue being at risk for developing motor dysfunctions.[22,23]

We reasoned that targeted gene delivery to the cervical spinal cord through intraspinal injection in *Gaa*$^{-/-}$ mice could provide insights into the potential contribution of CNS neuropathology to respiratory dysfunction. Therefore, we wished to determine if direct spinal injection of adeno-associated virus (AAV) encoding GAA would restore spinal GAA enzyme activity and whether such improvements would result in enhanced ventilation in adult *Gaa*$^{-/-}$ mice. The results of this study are consistent with the overall hypothesis that CNS pathology contributes to ventilatory dysfunction in *Gaa*$^{-/-}$ mice, and by extension, Pompe disease.

RESULTS

Distribution of AAV following intraspinal injection

Real-time quantitative PCR was used to measure the distribution of vector genome copies following injection of AAV5-GAA in *Gaa*$^{-/-}$ mice (**Figure 1a**). As expected, a high number of copies

Correspondence: *David D Fuller, Department of Physical Therapy, McKnight Brain Institute, University of Florida, College of Public Health and Health Professions, 100 S. Newell Dr., PO BOX 100154, Gainesville, Florida 32610, USA. E-mail: ddf@phhp.ufl.edu or Barry J Byrne, Department of Pediatrics, Powell Gene Therapy Center, University of Florida, College of Medicine, PO Box 100296, Gainesville, Florida 32610, USA. E-mail: bbyrne@ufl.edu*

© The American Society of Gene & Cell Therapy

(*i.e.*, >1 × 10^7 genome copies/μg of genomic DNA) were detected in the cervical spinal cord at or near the site of injection (C_3–C_8). Similarly robust levels were detected in spinal segments adjacent (C_1–C_2) or close to the injection (T_1–T_5). Much lower levels of vector genome copies (~1 × 10^5 genome copies/μg of genomic DNA) were detected in the medulla and at low thoracic and lumbar spinal levels, and AAV vector genomes were not detected in the diaphragm muscle. This is particularly important since it suggests that the altered ventilation following spinal cord injection in *Gaa*$^{-/-}$ mice (see below) resulted from transduction and restoration of GAA activity in the CNS but not the respiratory muscles.

A previous study described in detail the distribution of green fluorescent protein (GFP) expression following AAV5-GFP injection into the cervical spinal cord including both anterograde and retrograde transport properties.[24] In the present study, the primary purpose of the AAV5-GFP injections was to confirm AAV transduction of the region of the phrenic motor nucleus. GFP transduction was not exclusive to the ventral horn and expression was noted in neurons in both the intermediate and ventral cervical gray matter. However, GFP expression was most robust at the site of injection (*i.e.*, the ventral horn) and there was consistent transduction in the vicinity of the phrenic motor nucleus (**Figure 1b,c**). The neurons shown in **Figure 1b** are consistent with the appearance of phrenic motoneurons as evidenced by their distinctive location and the tight clustering of the cell bodies.[25] GFP labeling also was noted in ventral root axons indicating anterograde transport[26] (**Figure 1c**).

Intraspinal injection of AAV5-GAA restores GAA enzyme activity

En bloc segments of the cervical (C_3–C_5) and thoracic (T_5–T_8) spinal cord were harvested 4 weeks after spinal injection and GAA enzyme activity was assayed (**Figure 2a**). As expected,[19] GAA enzyme activity was negligible in *Gaa*$^{-/-}$ mice injected with AAV5-GFP. In contrast, spinal cords harvested after AAV5-GAA injection showed GAA activity levels that were comparable to values obtained from B6/129 mouse spinal cords. Indeed, evaluation of GAA activity using two-way analysis of variance revealed a very robust treatment effect ($P < 0.001$; **Figure 2a**). The normalization of GAA activity was not observed at more caudal spinal cord levels. Specifically,

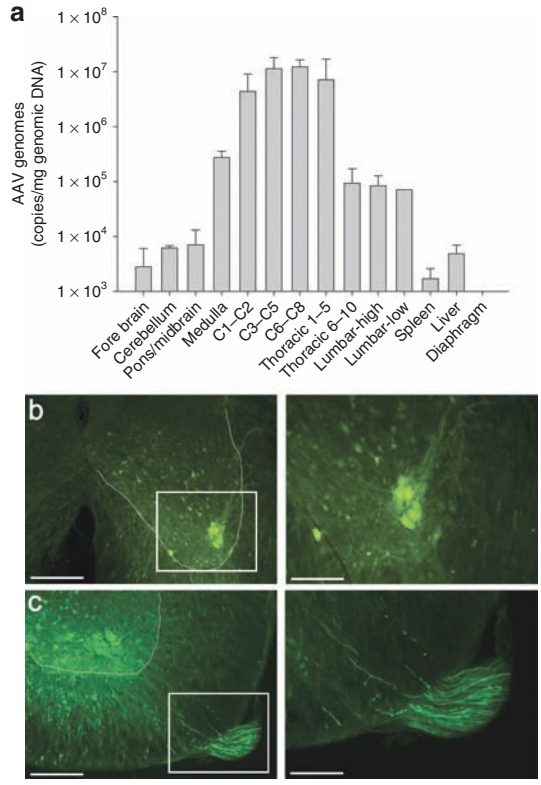

Figure 1 AAV distribution following spinal cord injection. (**a**) Quantitative real-time PCR was used to examine the distribution of AAV at 4 weeks postspinal cord injection. A robust number AAV vector genome copies was detected in the cervical and high thoracic (T_1–T_5) spinal cord. A smaller number of genomes were detected in the medulla and caudal thoracic cord region. Importantly, AAV could not be detected in the diaphragm muscle. (**b**) Robust GFP expression in a neuronal cluster in the C4 spinal cord in the approximate location of the phrenic motor nucleus, and (**c**) GFP expression throughout the ventral horn and also in C4 ventral root axons. The area indicated by the box in the left image is presented at a higher magnification in the image immediately to the right. The dashed line indicates the approximate outline of the ventral horn. Bars: 100 μm (lower power) and 50 μm (higher power).

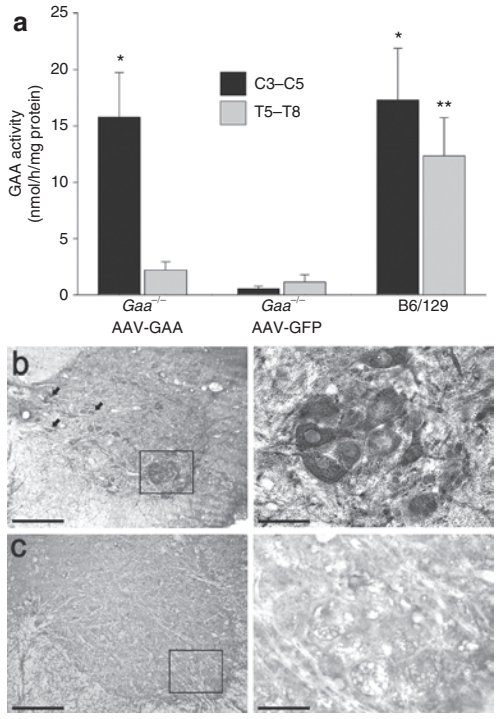

Figure 2 GAA activity in the spinal cord is restored following AAV5-GAA injection. (**a**) At 4 weeks postspinal injection, homogenates from the cervical (C_3–C_5) or thoracic spinal cord (T_5–T_8) were assayed for GAA enzyme activity. Following intraspinal AAV5-GAA injection, *Gaa*$^{-/-}$ mice showed cervical GAA activity comparable to what was observed in B6/129 mice. However, *Gaa*$^{-/-}$ mice receiving intraspinal AAV5-GFP had negligible cervical GAA activity. (**b**) Immunohistochemistry experiments revealed positive GAA staining in putative phrenic motoneurons (box) and cervical interneurons (arrows). (**c**) GAA immunostaining was absent in *Gaa*$^{-/-}$ mice receiving AAV5-GFP. In **b** and **c**, the area indicated by the box in the left image is presented at a higher magnification in the image immediately to the right. *$P < 0.05$ vs. corresponding AAV-GFP data point; **$P < 0.05$ vs. corresponding AAV-GFP and AAV5-GAA data points; Bars: 100 μm (lower power) and 50 μm (higher power).

© The American Society of Gene & Cell Therapy

GAA activity in lower thoracic segments (T_5–T_8) was minimal in both sham injected (AAV5-GFP) and AAV5-GAA treated *Gaa*$^{-/-}$ mice (**Figure 2a**). The biochemical assessment of GAA activity was supplemented with spinal cord immunohistochemistry to visualize enzyme distribution. *Gaa*$^{-/-}$ mice that had received AAV5-GAA injections showed GAA positive neurons in the region of the phrenic motor nucleus (cervical laminae IX) and also in interneurons[27,28] including cervical laminae VIII and VII (**Figure 2b**). GAA immunostaining was not detected in cervical or thoracic cords from *Gaa*$^{-/-}$ mice injected with AAV5-GFP (**Figure 2c**).

In other experiments, spinal cords were stained with the periodic acid Schiff (PAS) method to assess glycogen reaction product[29] (**Figure 3**). Two prior reports have established that PAS staining is robust in neurons throughout the ventral spinal cord in Pompe mice.[5,12] We found that PAS staining was absent or minimal at or near the site of spinal cord AAV5-GAA injection (**Figure 3a,b**). The lack of PAS staining suggests that neuronal glycogen storage was eliminated or reduced. In contrast, control regions in the thoracic spinal cord that were more distant from the injection site remained PAS positive (**Figure 3c,d**) and showed evidence of neuropathology consistent with prior reports in untreated Pompe mouse models.[5,12]

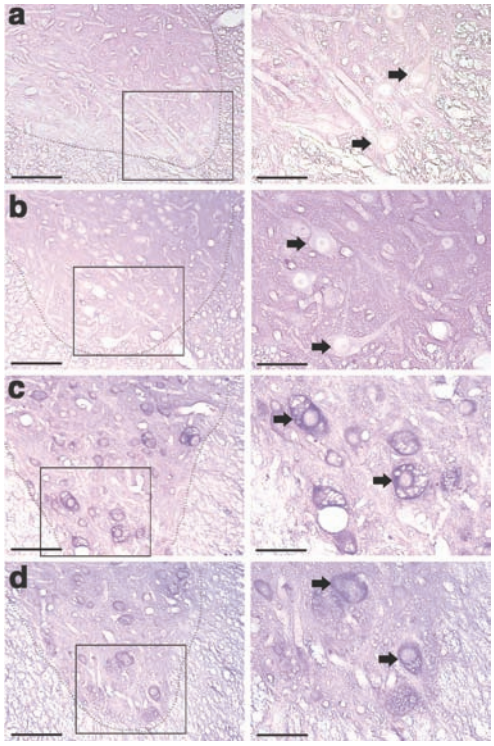

Figure 3 Histological evidence for glycogen clearance following spinal cord injection with AAV5-GAA. (**a–d**) 40 µm paraffin-embedded and PAS stained spinal cord sections from an adult *Gaa*$^{-/-}$ mouse obtained 1 month following cervical spinal injection with AAV5-GAA. The area indicated by the box in the left column is presented at a higher magnification in the image immediately to the right; arrows indicate neuronal cell bodies. Neuronal PAS staining is minimal at or near the site of AAV5-GAA injection (mid-cervical spinal cord, **a**,**b**). However, at sites more distant from the injection (mid-thoracic spinal cord, **c**,**d**) neuronal PAS staining and neuropathology is evident throughout the ventral horn. The dashed lines indicate the approximate outline of the cervical ventral horn. Bars: 100 µm (lower power) and 50 µm (higher power).

Enhanced ventilation in *Gaa*$^{-/-}$ mice following intraspinal AAV5-GAA injection

Ventilation was quantified during quiet, normoxic breathing (baseline), and a hypercapnic respiratory challenge (7% inspired CO_2) in unanesthetized mice using whole-body plethysmography (*e.g.*, **Figure 4a**). Ventilation was measured at 1, 2, and 4 months post-AAV injection in *Gaa*$^{-/-}$ mice to test the hypothesis that inspiratory tidal volume would be greater following injection of AAV5-GAA versus AAV5-GFP. During the baseline condition (**Figure 4b**, left panels), breathing frequency (breaths/min) was similar between groups (P = 0.152), and did not change across

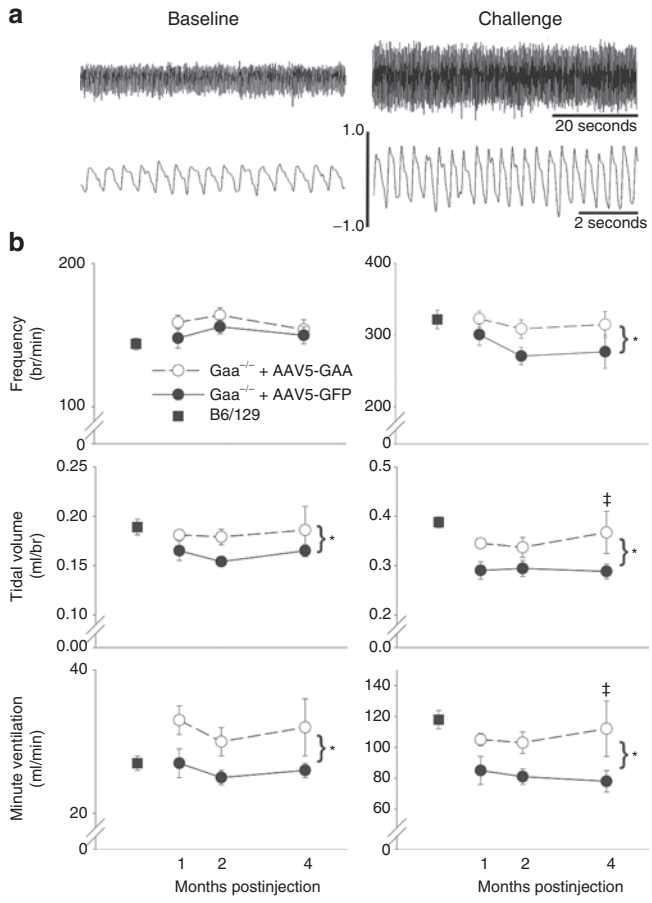

Figure 4 Ventilation in Gaa$^{-/-}$ mice after AAV injection. Inspiratory frequency (breaths/min), tidal volume (ml/breath), and inspired minute ventilation (ml/min) were measured at intervals following spinal AAV injection in unanesthetized mice using whole-body plethysmography. (**a**) Representative airflow traces during quiet breathing (baseline conditions of 21% O_2 with balance of N_2) and a hypercapnic respiratory challenge (7% inspired CO_2) are shown. Expanded traces in the lower portion of **a** are provided to illustrate individual breaths.Bars on the airflow traces are in ml/sec. (**b**) Group average ventilation data during baseline (left panels) and hypercapnic respiratory challenge (right panels) in *Gaa*$^{-/-}$ mice injected with AAV5-GAA (dashed lines) or AAV-GFP (solid lines), and B6/129 control mice (square symbol). Small but statistically significant differences in tidal volume and minute ventilation between AAV5-GAA vs. AAV5-GFP injected *Gaa*$^{-/-}$ mice were noted at baseline. More robust differences between these groups were seen during the hypercapnic respiratory challenge. *Indicates a significant overall difference between AAV5-GFP and AAV5-GAA injected *Gaa*$^{-/-}$ mice (two-way analysis of variance); ‡Indicates that the data point is significantly greater than corresponding AAV5-GFP data point.

© The American Society of Gene & Cell Therapy

time points ($P = 0.887$). However, mice treated with the AAV5-GAA had a small but statistically significant increase in baseline tidal volume ($P = 0.021$). Baseline tidal volume, however, did not differ across the three time points ($P = 0.870$). The elevated tidal volume after AAV5-GAA injection was associated with increases in the baseline minute ventilation of ~20% ($P = 0.006$). Minute ventilation was not different across time postinjection ($P = 0.994$). It should be noted that this change in ventilation has the potential to cause significant physiological changes in arterial blood gases during baseline breathing.[30] Lastly, the baseline ventilation measured in AAV5-GAA injected *Gaa*$^{-/-}$ mice at 4 months postinjection was not different than values obtained from age-matched B6/129 mice (**Figure 4b**, left panels, $P = 0.15$).

Differences in the overall pattern of breathing between AAV5-GFP versus AAV5-GAA injected mice were more prominent when the overall level of respiratory drive was increased by exposure to hypercapnia (**Figure 4b**, right panels). Indeed, both hypercapnic breathing frequency ($P = 0.014$) and tidal volume ($P = 0.002$) were greater in mice injected with AAV5-GAA. Hypercapnic minute ventilation also was greater in AAV5-GAA injected mice ($P < 0.001$). However, none of these variables showed a statistically significant difference across time postinjection (all $P > 0.272$). Thus, consistent with the biochemical GAA activity data (**Figure 2a**), the impact of the AAV5-GAA injection on ventilation was evident by 1 month postinjection and maintained over the next several months. The hypercapnic ventilation data also were normalized to the baseline output (%baseline). With this approach, no differences between AAV5-GAA versus. AAV5-GFP treated mice were noted in hypercapnic frequency ($P = 0.379$), tidal volume ($P = 0.154$), or ventilation ($P = 0.218$). This observation suggests that both groups of mice were able to respond to the respiratory challenge in a similar fashion, but the AAV5-GAA treated mice could achieve a higher absolute respiratory output. Ventilation during hypercapnia in *Gaa*$^{-/-}$ mice injected with AAV5-GAA was not different from ventilation measured in age-matched B6/129 mice (**Figure 4b**, right panels, $P = 0.67$).

DISCUSSION

These results contribute to the emerging body of evidence that neuropathology is a functionally relevant aspect of Pompe disease. Our most significant finding is that AAV5-GAA can mitigate glycogen accumulation in the spinal cord and reduce respiratory deficits in *Gaa*$^{-/-}$ mice. Indeed, intraspinal injection of AAV5-GAA to Pompe (*Gaa*$^{-/-}$) mice restored spinal GAA enzyme activity comparable to control tissue levels. Moreover, intraspinal gene delivery[24,31] was associated with enhanced ventilation despite the continued absence of GAA activity in the diaphragm muscle. Accordingly, our results support the hypothesis that CNS GAA deficiency impairs respiratory function, due to reduced respiratory motoneuron output.[5] We suggest that therapies targeting both the CNS and skeletal muscle may be necessary to treat respiratory-related dysfunction in Pompe disease.[5,32,33]

CNS pathology in Pompe disease and animal models

The progressive respiratory failure associated with Pompe disease has been attributed to respiratory muscle dysfunction.[34,35] Indeed, skeletal muscle pathology is evident in animal Pompe models[32,36,37] and both pediatric and adult Pompe patients.[1,38] Moreover, computed tomography imaging of the diaphragm in children with Pompe disease indicates a reduction in the overall mass of the diaphragm (B.J. Byrne, unpublished results). *Gaa*$^{-/-}$ mice have both attenuated ventilation and reduced diaphragm muscle contractility.[5,39,33] While impaired muscle function certainly contributes to respiratory insufficiency in Pompe disease, skeletal muscle obviously cannot function correctly without appropriate motoneuron input. The current data support the concept that motor deficits in Pompe disease are a significant part of the observed respiratory insufficiency.[5,8,10–12,14,17,33] In this regard, there have been a few clinical case reports suggesting an involvement of the CNS in motor[10,13–16] and possibly cognitive deficiencies.[40] In particular, reports of impaired or absent spinal reflexes in Pompe patients[10,14] are consistent with dysfunction in spinal circuits.[5,10] Pompe animal models also show considerable glycogen accumulation in the CNS.[5,11,12] Sidman and colleagues used PAS staining and biochemical methods to demonstrate robust accumulation of CNS glycogen in the $6^{neo}/6^{neo}$ mouse Pompe model.[12] CNS neuropathology was widespread, and spinal motoneurons showed considerable glycogen accumulation.[12] Similarly, we previously described glycogen accumulation in the cervical spinal cord and in retrogradely identified phrenic motoneurons in the *Gaa*$^{-/-}$ mouse model.[5]

These findings, along with the current data, are consistent with the hypothesis that Pompe respiratory deficits have spinal[5] and possibly a supraspinal component.[41] Following intraspinal injection, the highest expression of AAV was seen in the cervical spinal cord including the region containing the phrenic motor nucleus (*i.e.*, C_3–C_6).[28] The AAV5-GAA injection resulted in normalized spinal cord GAA activity and reduction in spinal PAS staining when assessed 1 month postinjection. Prior work suggests that AAV supports prolonged and possibly even permanent transgene expression following delivery to the CNS.[42,43] Accordingly, we hypothesize that the apparent reduction in spinal cord glycogen accumulation and associated neuropathology noted in our study lead to sustained increased phrenic motor output and improved ventilation. AAV vector genomes could be detected along the neuraxis, although we cannot definitively say if this reflects axonal transport[24] or diffusion from the injection site. Specifically, we found evidence for AAV transduction, *albeit* at reduced levels, in both the medulla and the thoracic spinal cord. It is, therefore, possible that the function of both the respiratory intercostal motoneurons and interneurons (thoracic spinal cord) and/or medullary respiratory control neurons and/or networks were influenced by the cervical spinal AAV injection. Medullary dysfunction is possible in *Gaa*$^{-/-}$ mice since we recently observed altered XII nerve output and increased variance in the timing of the respiratory cycle in these mice.[41] Accordingly, brainstem glycogen accumulation may directly alter function of the respiratory control circuitry (versus motoneuron dysfunction).

Significance

Current treatment by enzyme replacement therapy has been responsible for improving the overall survival in early onset Pompe disease.[44] For example, the 18 months survival rate of Pompe infants receiving systemic enzyme replacement therapy (ERT) is

© The American Society of Gene & Cell Therapy

dramatically increased compared to historical control patients.[1] However, variability in the success of ERT has been noted,[45] and the long-term survival rates and motor function capabilities of patients on ERT have not been carefully evaluated. In this regard, it is interesting that Muller and colleagues found that Pompe children on ERT are at high risk for developing speech disorders.[23] These authors speculated that this could reflect lower motoneuron involvement which will not be effectively targeted by ERT because recombinant GAA enzyme does not effectively cross the blood-brain-barrier.[20,21] Similarly, Burrow *et al.*[17] recently described a 2-year-old Pompe child who after 19 months of ERT showed "acute worsening of weakness, particularly of the extremities and diaphragm". These authors noted that their Pompe case report "offers strong evidence that storage in the nervous system can lead to a loss of motor neurons and to neuropathic weakness". Lastly, Rohrbach and colleagues reported that ERT effectively delayed the muscular progression of a Pompe infant over a 44 months period, but neurological symptoms including impaired language development remained.[40] Rohrbach *et al.* comment on the "importance of close neurological follow-up" in Pompe patients receiving ERT. Thus, much evidence supports the view that intravenous GAA delivery may target cardiac and skeletal muscle,[46,47] but will not effectively mitigate CNS glycogen accumulation. This point is highlighted by our recent study in which an infant with Pompe disease had received ERT from a few months of age and showed considerable glycogen accumulation in the cervical spinal cord on postmortem examination.[5]

Based on the current data and both recent[5,12,17,18,23] and historical reports,[6,7,14] we hypothesize that therapy targeting both skeletal muscle and the CNS may be required to fully correct respiratory-related deficits. It also is important to emphasize that in the face of generalized weakness, the associated problems of diminished pharyngeal tone, limited secretion clearance, and ineffective cough all culminate in respiratory failure. New therapeutic options in Pompe disease could target a reduction in CNS glycogen storage or could provide a means of pharmacologically activating endogenous gene products. Another promising method to restore GAA activity to both muscle and neuronal tissue will be the use of AAV for gene transfer to muscle coupled with retrograde gene delivery to motor neurons.[39] Recently, an open label, Phase I/II study administering rAAV2/1-CMV-hGAA to the diaphragm by direct intramuscular injection has been initiated in children with Pompe disease (ClinicalTrials.gov Identifier: NCT00976352). The study is designed to target those on assisted ventilation with the most life-threatening complication of Pompe disease following partial effectiveness of ERT. Additional AAV serotypes which are potentially capable of more robust retrograde transduction (*i.e.*, muscle-to-motoneuron) may be candidates for future studies. Clinical application of gene transfer strategies, alone or in combination with ERT, may provide an important advancement in treatment of Pompe disease.

MATERIALS AND METHODS

Animals. B6/129 (N = 19) and $Gaa^{-/-}$ mice (N = 66) were used in this work, and the University of Florida's Institutional Animal Care and Use Committee approved all procedures. At the time of spinal cord injection, $Gaa^{-/-}$ mice given AAV5-GAA were 174 ± 3 days old and $Gaa^{-/-}$ mice injected with AAV5-GFP were of similar age (167 ± 14 days). The $Gaa^{-/-}$ mouse was generated by disruption of exon 6 and maintained on a C57BL/6× 129X1/SvJ backgroundv as described previously.[5,19] The B6/129 mice were originally obtained from Taconic (Hudson, NY) and then maintained at the University of Florida.

AAV vectors. The spinal cord was injected (see below) with AAV vectors that included single-stranded AAV5-Chicken β-actin 300 bp deletion-GAA (AAV5-CBAd300-GAA) (4.22×10^{13} vg/ml) or single-stranded AAV5-CBA-GFP (4.5×10^{13} vg/ml). A total of 35 $Gaa^{-/-}$ mice received AAV5-GAA and 31 $Gaa^{-/-}$ mice received AAV5-GFP. All vectors were generated and titered at the University of Florida Powell Gene Therapy Center Vector Core Lab using previously published methods.[48] Vectors were purified by iodixanol gradient centrifugation and anion-exchange chromatography as described in detail by Zolotukhin *et al.*[48] Final formulations of AAV5-CBAd300-GAA and AAV5-CBA-GFP vectors were in lactated ringer's.

Spinal cord injection. Mice were anesthetized with inhaled isoflurane (2–3% in O_2) and then placed in a stereotaxic frame (David Kopf Instruments, Tujunga, CA). Anesthesia was maintained *via* a nose cone throughout the surgical procedure. The cervical vertebral column was then exposed and a laminectomy was performed over the C_3–C_4 segments. Following a dural incision, spinal injections were made using glass micropipettes (tip diameter ~50 µm) and a pressure microinjection system (Picospritzer 2; Parker-Hannifin, Cleveland, OH). Injections were targeted to the phrenic motor nucleus based on our prior anatomical description.[25] Briefly, 2–3 bilateral, 0.5 µl injections were made 0.7 mm lateral to the spinal midline at a depth of 0.9–1.0 mm from the dorsal surface of the spinal cord. The surgical site was then closed and mice were given buprenorphine at ~12-hour intervals for 36 hours (0.1 mg/kg, intraperitoneally).

Genomic DNA extraction and real-time PCR. PCR was used to measure the distribution of AAV genomes from AAV5-GAA at 4 weeks following cervical spinal AAV injection in $Gaa^{-/-}$ mice (N = 3), and also to genotype a subset of the $Gaa^{-/-}$ mice. At 1 month postspinal AAV injection, tissues were harvested in a manner that prevented cross-contamination, snap frozen in liquid nitrogen and stored at −80 °C until genomic DNA (gDNA) was extracted. gDNA was isolated using a DNeasy blood and tissue kit (Qiagen, Valencia, CA) according to the manufacturer's instructions. gDNA concentrations were determined using an Eppendorf Biophotometer (Eppendorf, Hamburg, Germany). AAV genome copies in the gDNA were quantified by real-time PCR using an ABI 7900 HT sequence detection system (Applied Biosystems, Carlsbad, CA) according to the manufacturer's instructions and results were analyzed using the SDS 2.3 software. Briefly, primers and probe were designed to the SV40 poly-A region of the AAV vector as previously described.[32] A standard curve was performed using plasmid DNA containing the same SV40 poly-A target sequence. PCR reactions contained a total volume of 100 µl and were run at the following conditions: 50 °C for 2 minutes, 95 °C for 10 minutes, and 45 cycles of 95 °C for 15 seconds and 60 °C for 1 minute.

DNA samples were assayed in triplicate. In order to assess PCR inhibition, the third replicate was spiked with plasmid DNA at a ratio of 100 copies/µg gDNA. If this replicate was greater than 40 copies/µg gDNA then the results were considered acceptable. If a sample contained greater than or equal to 100 copies/µg gDNA it was considered positive for vector genomes. If a sample contained less than 100 copies/µg gDNA it was considered negative for vector genomes. If less than 1 µg of gDNA was analyzed to avoid PCR inhibition, the vector copy number reported was normalized per µg gDNA and the plasmid spike-in was reduced to maintain the ratio of 100 copies/µg gDNA.

$Gaa^{-/-}$ genotyping was done to confirm the absence of *Gaa* as described previously.[19,39] Briefly, DNA was isolated from tail snips and amplified using primers to exons 5 and 7 of the mouse GAA gene. A 692 bp product indicated the wild-type allele and a 2 kb product confirmed the insertion of a *neo* cassette and confirmed $Gaa^{-/-}$ mice.

© The American Society of Gene & Cell Therapy

GAA activity assay. These procedures were adapted from our prior report.[36] Spinal tissues were harvested from B6/129 mice, and *Gaa*$^{-/-}$ mice spinally injected with either AAV5-GAA or AAV5-GFP ($N = 4$ per group). Mice were euthanized *via* intraperitoneal injection of sodium pentobarbital (100 mg/kg, intraperitoneally) and *en bloc* spinal cord segments C_3–C_5 and T_5–T_8 were immediately harvested, frozen in liquid N_2 and maintained at −80 °C until biochemical analyses were performed. Briefly, tissues were homogenized in water and subjected to three freeze-thaw cycles. Homogenates were centrifuged at 14,000 rpm for 10 minutes at 4 °C and the resulting supernatant was assayed for GAA activity by measuring cleavage of 4-methylumbelliferyl-α-D-glucopyranoside after incubation for 1 hour at 37 °C. Protein concentration was measured using the Bio-Rad DC protein assay kit per manufacturer's instructions. Data are expressed relative to values measured in untreated GAA tissue levels (% control).

Histology and immunostaining. Qualitative assessment of spinal cord glycogen was done using the PAS method.[5,12,29] *Gaa*$^{-/-}$ mice ($N = 5$) were anesthetized with sodium pentobarbital (50 mg/kg, intraperitoneally) and then perfused through the heart with 4% paraformaldehyde in phosphate-buffered saline. Spinal cords were then harvested and postfixed overnight in the same solution. Spinal cords were embedded in paraffin, sectioned (10 µm), and stained with PAS as described previously.[5] In additional experiments, spinal cords were sectioned using a cryostat (40 µm), and immunohistochemical methods were used to visualize spinal GAA enzyme content. Briefly, tissues were incubated overnight (4 °C) in a 1:2,000 dilution of rabbit polyclonal GAA antibody (Covance, Emeryville, CA). Sections were then washed in phosphate-buffered saline (3×) and then exposed to a biotin-conjugated secondary antibody (1:200 dilution) at room temperature for 2 hours. Sections were then washed in phosphate-buffered saline (3×), incubated in an avidin-biotin complex (1 hour) and then reacted with 3,3′-diaminobenzidine tetrahydrochloride (DAB) for detection *via* light microscopy.

Ventilation measurements. Ventilation was quantified using whole-body plethysmography in unrestrained and unanesthetized mice as previously described.[5] Initial experiments were conducted using *Gaa*$^{-/-}$ mice that had received spinal injection of AAV5-GAA ($N = 22$) or AAV5-GFP ($N = 13$). Data were collected at three intervals postspinal injection as follows. In AAV5-GAA treated mice, ventilation was measured at 32 ± 1, 66 ± 3, and 128 ± 6 days postinjection. In AAV5-GFP treated mice, ventilation was measured at similar intervals of 31 ± 2, 69 ± 5, and 133 ± 9 days postinjection. These time points are subsequently designated as 1, 2, and 4 months postinjection, respectively. Additional plethysmography experiments were done in control B6/129 mice ($N = 16$; 277 ± 13 days of age). These B6/129 mice were not studied at multiple time points, and were evaluated to provide a comparison to the *Gaa*$^{-/-}$ mice at 4 months post-AAV injection.

To obtain the ventilation measurements, mice were placed inside a 3.5" × 5.75" Plexiglas chamber which was calibrated with known airflow and pressure signals before data collection. Data were collected in 10-s bins and the Drorbaugh and Fenn equation[49] was used to calculate respiratory volumes including tidal volume and minute ventilation. During both a 30 minutes acclimation period and subsequent 30–60 minutes baseline period mice breathed normoxic air (21% O_2, 79% N_2). At the conclusion of the baseline period, the mice were exposed to a brief respiratory challenge which consisted of a 10 minutes hypercapnic exposure (7% CO_2, balance O_2).

Breathing was assessed in both male and female mice, and χ^2 analyses indicated no effect of gender on any of the respiratory parameters ($P > 0.05$). Accordingly, male and female ventilation data were pooled. There was a tendency for AAV5-GAA mice to have greater body weight compared to those injected with AAV5-GFP ($P = 0.067$). Since body mass can influence metabolism and ventilation, we used a Spearman-Rho nonparametric correlation test to examine the relationship between the plethysmography data and body weight. No significant relationships between body weight and tidal volume, minute ventilation, or respiratory frequency (*i.e.*, breaths/min) data were observed (all $P > 0.265$). Accordingly, the plethysmography data are presented as absolute values (*i.e.*, ml) instead of dividing the respiratory volumes by body weight.[50]

Statistical analyses. The ventilation data were compared between AAV5-GAA and AAV5-GFP injected *Gaa*$^{-/-}$ mice using two-way analysis of variance. Comparisons to B6/129 mice were made using an unpaired *t*-test. GAA enzyme activity data were compared between groups using a two-way analysis of variance. Data were considered to be statistically different when $P < 0.05$.

ACKNOWLEDGMENTS

This work was supported by the National Institutes of Health Grants 1R01HD052682-01A1 (D.D.F.); HL59412 (B.J.B.); 5F32HL095282-02 (D.J.F.); NIDDK P01 DK58327 (B.J.B.). B.J.B., D.D.F., The Johns Hopkins University, and the University of Florida could be entitled to patent royalties for inventions described in this manuscript.

REFERENCES

1. Byrne, BJ, Kishnani, PS, Case, LE, Merlini, L, Müller-Felber, W, Prasad, S *et al.* (2011). Pompe disease: design, methodology, and early findings from the Pompe Registry. *Mol Genet Metab* **103**: 1–11.
2. Kishnani, PS, Corzo, D, Nicolino, M, Byrne, B, Mandel, H, Hwu, WL *et al.* (2007). Recombinant human acid [alpha]-glucosidase: major clinical benefits in infantile-onset Pompe disease. *Neurology* **68**: 99–109.
3. Hirschhorn, RR and Reuser, AJ (2000). Glycogen storage disease type II: acid alpha-glucosidase (acid maltase) deficiency. In: Scriver, CR, Beaudet, AL, Sly, WS and Valle, D (eds). *Metabolic Basis of Inherited Disease.* McGraw Hill: New York. pp. 3389–3420.
4. Raben, N, Plotz, P and Byrne, BJ (2002). Acid alpha-glucosidase deficiency (glycogenosis type II, Pompe disease). *Curr Mol Med* **2**: 145–166.
5. DeRuisseau, LR, Fuller, DD, Qiu, K, DeRuisseau, KC, Donnelly, WH Jr, Mah, C *et al.* (2009). Neural deficits contribute to respiratory insufficiency in Pompe disease. *Proc Natl Acad Sci USA* **106**: 9419–9424.
6. Gambetti, P, DiMauro, S and Baker, L (1971). Nervous system in Pompe's disease. Ultrastructure and biochemistry. *J Neuropathol Exp Neurol* **30**: 412–430.
7. Mancall, EL, Aponte, GE and Berry, RG (1965). Pompe's disease (diffuse glycogenosis) with neuronal storage. *J Neuropathol Exp Neurol* **24**: 85–96.
8. Martin, JJ, de Barsy, T, van Hoof, F and Palladini, G (1973). Pompe's disease: an inborn lysosomal disorder with storage of glycogen. A study of brain and striated muscle. *Acta Neuropathol* **23**: 229–244.
9. Martini, C, Ciana, G, Benettoni, A, Katouzian, F, Severini, GM, Bussani, R *et al.* (2001). Intractable fever and cortical neuronal glycogen storage in glycogenosis type 2. *Neurology* **57**: 906–908.
10. Teng, YT, Su, WJ, Hou, JW and Huang, SF (2004). Infantile-onset glycogen storage disease type II (Pompe disease): report of a case with genetic diagnosis and pathological findings. *Chang Gung Med J* **27**: 379–384.
11. Matsui, T, Kuroda, S, Mizutani, M, Kiuchi, Y, Suzuki, K and Ono, T (1983). Generalized glycogen storage disease in Japanese quail (Coturnix coturnix japonica). *Vet Pathol* **20**: 312–321.
12. Sidman, RL, Taksir, T, Fidler, J, Zhao, M, Dodge, JC, Passini, MA *et al.* (2008). Temporal neuropathologic and behavioral phenotype of 6neo/6neo Pompe disease mice. *J Neuropathol Exp Neurol* **67**: 803–818.
13. Clement, DH and Godman, GC (1950). Glycogen disease resembling mongolism, cretinism, and amytonia congenita; case report and review of literature. *J Pediatr* **36**: 11–30, illust.
14. Hogan, GR, Gutmann, L, Schmidt, R and Gilbert, E (1969). Pompe's disease. *Neurology* **19**: 894–900.
15. Willemsen, MA, Jira, PE, Gabreëls, FJ, van der Ploeg, AT and Smeitink, JA (1998). [Three hypotonic neonates with hypertrophic cardiomyopathy: Pompe's disease]. *Ned Tijdschr Geneeskd* **142**: 1388–1392.
16. Zellweger, H, Dark, A and Abu-Haidar, GA (1955). Glycogen disease of skeletal muscle; report of two cases and review of literature. *Pediatrics* **15**: 715–732.
17. Burrow, TA, Bailey, LA, Kinnett, DG and Hopkin, RJ (2010). Acute progression of neuromuscular findings in infantile Pompe disease. *Pediatr Neurol* **42**: 455–458.
18. Rohrbach, M, Klein, A, Köhli-Wiesner, A, Veraguth, D, Scheer, I, Balmer, C *et al.* (2010). CRIM-negative infantile Pompe disease: 42-month treatment outcome. *J Inherit Metab Dis* **33**: 751–757.
19. Raben, N, Nagaraju, K, Lee, E, Kessler, P, Byrne, B, Lee, L *et al.* (1998). Targeted disruption of the acid alpha-glucosidase gene in mice causes an illness with critical features of both infantile and adult human glycogen storage disease type II. *J Biol Chem* **273**: 19086–19092.
20. Kikuchi, T, Yang, HW, Pennybacker, M, Ichihara, N, Mizutani, M, Van Hove, JL *et al.* (1998). Clinical and metabolic correction of pompe disease by enzyme therapy in acid maltase-deficient quail. *J Clin Invest* **101**: 827–833.
21. Raben, N, Danon, M, Gilbert, AL, Dwivedi, S, Collins, B, Thurberg, BL *et al.* (2003). Enzyme replacement therapy in the mouse model of Pompe disease. *Mol Genet Metab* **80**: 159–169.
22. Jones, HN, Muller, CW, Lin, M, Banugaria, SG, Case, LE, Li, JS *et al.* (2010). Oropharyngeal dysphagia in infants and children with infantile Pompe disease. *Dysphagia* **25**: 277–283.
23. Muller, CW, Jones, HN, O'Grady, G, Suarez, AH, Heller, JH and Kishnani, PS (2009). Language and speech function in children with infantile Pompe disease. *J Pediatr Neurol* **7**: 147–156.

© The American Society of Gene & Cell Therapy

24. Burger, C, Gorbatyuk, OS, Velardo, MJ, Peden, CS, Williams, P, Zolotukhin, S *et al.* (2004). Recombinant AAV viral vectors pseudotyped with viral capsids from serotypes 1, 2, and 5 display differential efficiency and cell tropism after delivery to different regions of the central nervous system. *Mol Ther* **10**: 302–317.
25. Qiu, K, Lane, MA, Lee, KZ, Reier, PJ and Fuller, DD (2010). The phrenic motor nucleus in the adult mouse. *Exp Neurol* **226**: 254–258.
26. Chamberlin, NL, Du, B, de Lacalle, S and Saper, CB (1998). Recombinant adeno-associated virus vector: use for transgene expression and anterograde tract tracing in the CNS. *Brain Res* **793**: 169–175.
27. Lane, MA, White, TE, Coutts, MA, Jones, AL, Sandhu, MS, Bloom, DC *et al.* (2008). Cervical prephrenic interneurons in the normal and lesioned spinal cord of the adult rat. *J Comp Neurol* **511**: 692–709.
28. Qiu, K, Lane, MA, Lee, KZ, Reier, PJ and Fuller, DD (2010). The phrenic motor nucleus in the adult mouse. *Exp Neurol* **226**: 254–258.
29. Guth, L and Watson, PK (1968). A correlated histochemical and quantitative study on cerebral glycogen after brain injury in the rat. *Exp Neurol* **22**: 590–602.
30. Hlastala, MP and Berger, AJ (2001). *Physiology of Respiration.* Oxford University Press: New York. pp. 65–80.
31. Peel, AL, Zolotukhin, S, Schrimsher, GW, Muzyczka, N and Reier, PJ (1997). Efficient transduction of green fluorescent protein in spinal cord neurons using adeno-associated virus vectors containing cell type-specific promoters. *Gene Ther* **4**: 16–24.
32. Mah, CS, Falk, DJ, Germain, SA, Kelley, JS, Lewis, MA, Cloutier, DA *et al.* (2010). Gel-mediated delivery of AAV1 vectors corrects ventilatory function in Pompe mice with established disease. *Mol Ther* **18**: 502–510.
33. Mah, CS, Falk, DJ, Germain, SA, Kelley, JS, Lewis, MA, Cloutier, DA*et al.* (2010). Gel-mediated delivery of AAV1 vectors corrects ventilatory function in Pompe mice with established disease. *Mol Ther* **18**: 502–510.
34. Burghaus, L, Liu, W, Neuen-Jacob, E, Gempel, K and Haupt, WF (2006). [Glycogenesis Type II (M. Pompe). Selective failure of the respiratory musculature–a rare first symptom]. *Nervenarzt* **77**: 181–2, 185–186.
35. Pellegrini, N, Laforet, P, Orlikowski, D, Pellegrini, M, Caillaud, C, Eymard, B *et al.* (2005). Respiratory insufficiency and limb muscle weakness in adults with Pompe's disease. *Eur Respir J* **26**: 1024–1031.
36. Fraites, TJ Jr, Schleissing, MR, Shanely, RA, Walter, GA, Cloutier, DA, Zolotukhin, I *et al.* (2002). Correction of the enzymatic and functional deficits in a model of Pompe disease using adeno-associated virus vectors. *Mol Ther* **5**(5 Pt 1): 571–578.
37. Rucker, M, Fraites, TJ Jr, Porvasnik, SL, Lewis, MA, Zolotukhin, I, Cloutier, DA *et al.* (2004). Rescue of enzyme deficiency in embryonic diaphragm in a mouse model of metabolic myopathy: Pompe disease. *Development* **131**: 3007–3019.
38. Kishnani, PS and Howell, RR (2004). Pompe disease in infants and children. *J Pediatr* **144** (suppl. 5): S35–S43.
39. Mah, C, Pacak, CA, Cresawn, KO, Deruisseau, LR, Germain, S, Lewis, MA *et al.* (2007). Physiological correction of Pompe disease by systemic delivery of adeno-associated virus serotype 1 vectors. *Mol Ther* **15**: 501–507.
40. Rohrbach, M, Klein, A, Kohli-Wiesner, A, Veraguth, D, Scheer, I, Balmer, C *et al.* (2010). CRIM-negative infantile Pompe disease: 42-month treatment outcome. *J Inherit Metab Dis* **33**: 751–757.
41. Lee, KZ, Qiu, K, Sandhu, MS, Elmallah, MK, Falk, DJ, Lane, MA *et al.* (2011). Hypoglossal neuropathology and respiratory activity in pompe mice. *Front Physiol* **2**: 31.
42. Bankiewicz, KS, Forsayeth, J, Eberling, JL, Sanchez-Pernaute, R, Pivirotto, P, Bringas, J *et al.* (2006). Long-term clinical improvement in MPTP-lesioned primates after gene therapy with AAV-hAADC. *Mol Ther* **14**: 564–570.
43. Mandel, RJ, Manfredsson, FP, Foust, KD, Rising, A, Reimsnider, S, Nash, K *et al.* (2006). Recombinant adeno-associated viral vectors as therapeutic agents to treat neurological disorders. *Mol Ther* **13**: 463–483.
44. Beck, M (2010). Therapy for lysosomal storage disorders. *IUBMB Life* **62**: 33–40.
45. Van den Hout, JM, Kamphoven, JH, Winkel, LP, Arts, WF, De Klerk, JB, Loonen, MC *et al.* (2004). Long-term intravenous treatment of Pompe disease with recombinant human alpha-glucosidase from milk. *Pediatrics* **113**: e448–e457.
46. Levine, JC, Kishnani, PS, Chen, YT, Herlong, JR and Li, JS (2008). Cardiac remodeling after enzyme replacement therapy with acid alpha-glucosidase for infants with Pompe disease. *Pediatr Cardiol* **29**: 1033–1042.
47. Sugai, F, Kokunai, Y, Yamamoto, Y, Hashida, G, Shimazu, K, Mihara, M *et al.* (2010). Use of the muscle volume analyzer to evaluate enzyme replacement therapy in late-onset Pompe disease. *J Neurol* **257**: 461–463.
48. Zolotukhin, S, Potter, M, Zolotukhin, I, Sakai, Y, Loiler, S, Fraites, TJ Jr *et al.* (2002). Production and purification of serotype 1, 2, and 5 recombinant adeno-associated viral vectors. *Methods* **28**: 158–167.
49. Drorbaugh, JE and Fenn, WO (1955). A barometric method for measuring ventilation in newborn infants. *Pediatrics* **16**: 81–87.
50. Packard GC, Boardman, TJ (1999). The use of percentages and size-specific indices to normalize physiological data for variation in body size: wasted time, wasted effort? *Comp Biochem Physiol A Mol Integr Physiol* **122**: 37–44.